

1 **Oxidation-reduction potential (ORP) as a tool for process monitoring**  
2 **of H<sub>2</sub>O<sub>2</sub>/LPMO assisted enzymatic hydrolysis of cellulose**

3

4 Adnan Kadić<sup>a,1</sup>, Piotr Chylenski<sup>b</sup>, Mads Anders Tengstedt Hansen<sup>c,2</sup>, Oskar Bengtsson<sup>c</sup>, Vincent  
5 G.H. Eijssink<sup>b</sup>, Gunnar Lidén<sup>a</sup>

6

7 <sup>a</sup>Department of Chemical Engineering, Lund University, P.O. Box 118, SE-221 00 Lund,  
8 Sweden

9 <sup>b</sup>Faculty of Chemistry, Biotechnology and Food Science, Norwegian University of Life  
10 Sciences (NMBU), P.O. Box 5003, NO-1432 Ås, Norway

11 <sup>c</sup>Borregaard A/S, P.O. Box 162, NO-1701 Sarpsborg, Norway

12

13 <sup>1</sup>Corresponding author: adnan.kadic@chemeng.lth.se

14 <sup>2</sup>Present address: Danish Technological Institute, Gregersensvej 8, DK-2630, Taastrup,  
15 Denmark

16

17 **Conflicts of interest**

18 None declared.

19 **Acknowledgements**

20 This study was part of the project “Value Added Sugar Platform” financed by the Research  
21 Council of Norway, project 256766. The authors thank Novozymes A/S for providing enzymes  
22 used.

1 **Abstract**

2 Oxidation-reduction potential (ORP) is an environmental factor of importance in several  
3 biological conversion processes. Lytic polysaccharide monooxygenases (LPMOs)  
4 catalyze oxidative disruption of the cellulose chain in the presence of oxygen or  
5 hydrogen peroxide and increase enzymatic hydrolysis yields. However, the enzymes are  
6 also sensitive to oxidative damage and the level of oxidative agent needs to be  
7 controlled to avoid inactivation of the LPMOs. In the current study, enzymatic  
8 hydrolysis of sulfite-pretreated softwood (12% DM loading) was carried out in lab scale  
9 reactors with gradual addition of hydrogen peroxide using an LPMO-containing  
10 commercial enzyme cocktail. The ORP was measured during enzymatic hydrolysis  
11 together with released glucose and the level of C4-oxidized dimer as a marker for  
12 LPMO activity. Arrests in LPMO activity coincided with a markedly changed ORP  
13 signal and this was utilized in subsequent experiments in which the feed rate of  
14 hydrogen peroxide was controlled by keeping the ORP at predetermined set-points of -  
15 40 mV, -80 mV and -120 mV. Under anaerobic conditions, the highest hydrolysis yield  
16 (78% after 72 h) was found for the ORP set-point of -80 mV. The results show that  
17 ORP can serve as an indicator of LPMO activity and may help optimizing overall  
18 process efficiency.

19

20

21

22 Keywords: cellulose, enzymatic hydrolysis, lytic polysaccharide monooxygenase  
23 (LPMO), oxidation-reduction potential (ORP), hydrogen peroxide, redox

## 1 **1. Introduction**

2 Efficient production of biofuels and biochemicals from lignocellulosic biomass is  
3 needed in order to establish a future low-carbon economy. Although the cost of the  
4 enzymatic hydrolysis of cellulose has come down quite significantly in recent years, it  
5 is still substantial and further cost reductions are needed to reach cost levels for  
6 cellulosic sugars comparable to those of starch derived sugars. Overcoming the  
7 recalcitrance of the cellulosic substrate by better utilizing the activity of lytic  
8 polysaccharide monooxygenases (LPMOs) present in commercial enzyme cocktails is  
9 one highly promising approach towards this goal.

10 The oxidative activity of LPMOs was first discovered in chitin-acting enzymes [1],  
11 closely followed by reports on cellulose acting enzymes [2–5]. The main findings of  
12 these early studies were: (1) LPMOs incorporate a single oxygen atom into the  
13 polysaccharide chain during oxidative cleavage, (2) LPMO activity requires electron  
14 donors (such as ascorbate) and (3) the catalytic center of LPMOs contains a copper ion.  
15 Subsequently, it was shown that lignin and/or lignin degradation products can serve as  
16 electron donors, eliminating the need for the addition of external electron donors during  
17 enzymatic hydrolysis of pretreated biomass [6–9]. Additionally, the importance of  
18 dissolved oxygen was confirmed by the fact that anaerobic conditions did not support  
19 LPMO activity [9,10].

20 The exact mechanism of LPMO action is still not fully elucidated. Recent results  
21 indicate that  $H_2O_2$  is a co-substrate for the oxidation of cellulose by LPMOs [11]. Under  
22 aerobic conditions LPMOs that are not bound to substrate generate  $H_2O_2$  from  
23 stoichiometric amounts of oxygen and reducing agent [12], and this could fuel  $H_2O_2$ -  
24 driven cellulose cleavage. A recent study has shown that continuous feeding of  $H_2O_2$  to

1 saccharification reactions with Cellic CTec2 increases the rate of cellulose oxidation,  
2 without the need for stoichiometric addition of reducing agent [13]. These recent  
3 developments open up for new process alternatives in commercial hydrolysis of  
4 cellulose, in which hydrogen peroxide is used as the oxidant, either together with or  
5 instead of oxygen, to increase the rate of hydrolysis and/or ultimate glucose yields.

6 One key problem related to the use of LPMOs in biomass processing is their sensitivity  
7 to inactivation by oxidative damage. It is well known that  $H_2O_2$  may damage enzymes,  
8 likely through generation of hydroxyl radicals upon reactions with transition metals, and  
9 it has been shown that enzyme inactivation during biomass processing may be  
10 alleviated by addition of catalases [14]. In this respect, LPMOs are special because their  
11 inactivation does not primarily result from these general processes but from a highly  
12 specific auto-catalytic process that only damages the LPMO [11]. This process, which  
13 leads to oxidative damage in the catalytic center of the LPMO [11], emerges when a  
14 reduced LPMO reacts with  $H_2O_2$  in the absence of substrate. Thus, the rate of LPMO  
15 inactivation depends on the availability of both the polysaccharide substrate and the  
16 concentration of  $H_2O_2$  [11,15], pointing to a need to control the levels of dissolved  $O_2$   
17 and/or  $H_2O_2$  during enzymatic hydrolysis.

18 The potential of an electrode immersed in a solution can be taken as a measure of  
19 oxidizing or reducing conditions and referred to as the oxidation-reduction potential  
20 (ORP). The equilibrium cell potential is determined by the activities of the substances  
21 that are oxidized or reduced and can be calculated using the Nernst equation [16].  
22 However, in practice this is difficult for complex systems. Thus, the most common  
23 approach used in process conditions is to directly measure the potential of an inert metal  
24 electrode (typically platinum) immersed in a solution of interest. The resulting ORP

1 measurements have been used for monitoring and control of various redox processes,  
2 including biological [17] and chemical wastewater treatment [18], and microbial  
3 fermentation [19,20].

4 The objective of the present study was to assess the usefulness of continuous *in situ*  
5 ORP measurements with a platinum electrode as a means to follow LPMO activity  
6 during enzymatic hydrolysis of an industrial cellulosic substrate. Furthermore, the  
7 effects of controlling the ORP at specific set-point values by feed-back regulated  
8 addition of hydrogen peroxide were examined under both anaerobic and aerobic  
9 conditions. The substrate used in the study was sulfite-pretreated Norway spruce, and  
10 hydrolysis was obtained with a commercial cellulase preparation (Cellic CTec3).

## 11 **2. Materials and methods**

### 12 **2.1. Biomass pretreatment and composition analysis**

13 Norway spruce (*Picea abies*) was pretreated by Borregaard AS (Sarpsborg, Norway).  
14 The pretreatment included a sulfite cooking step, which converts lignin into water  
15 soluble lignosulfonates and most of the hemicellulose into monosaccharides (the  
16 composition of the resulting cellulose-enriched material is shown in Table 1). The  
17 monosaccharides released during the pretreatment and the enzymatic hydrolysis  
18 described below were mostly D-glucose, D-mannose, D-xylose, D-galactose and L-  
19 arabinose, which, in the remainder of the text are referred to without the enantiomer  
20 prefix.

21 The pretreated solids were washed and then dewatered using a Strainpress SP4 screw  
22 press (HUBER SE, Berching, Germany). The liquid fraction from the pretreatment,  
23 referred to as spent sulfite liquor (SSL), was collected. The SSL and the solid pretreated

1 spruce material were kept stored at 4 °C until further use. Additional information on the  
2 pretreatment process is proprietary information of Borregaard A/S.

3 The pretreated spruce solids were water-insoluble solids (WIS), while SSL contained  
4 water-soluble solids (WSS). The dry matter (DM) content was determined by drying at  
5 105 °C for 24 hours. The DM contents of the pretreated spruce solids and SSL were  
6 35.1±0.4% and 13.30±0.03%, respectively. The composition of the pretreated spruce  
7 solids and the SSL was analyzed according to NREL (National Renewable Energy  
8 Laboratories) standard procedures [21,22], and is shown in Table 1.

## 9 **2.2. LPMO reactions with SSL as reductant**

10 *Thermoascus aurantiacus* LPMO (*TaAA9A*) was expressed in *Pichia pastoris* and  
11 purified essentially as described before [23]. Purified LPMO was saturated with Cu (II)  
12 by incubation with CuSO<sub>4</sub> (3:1 molar ratio of copper:enzyme) for 30 min at room  
13 temperature [24]. Subsequently, the protein solution was loaded onto a PD midiTrap G-  
14 25 desalting column (GE Healthcare, UK), equilibrated with 50 mM Bis-Tris/HCl  
15 buffer pH 6.5. Protein was eluted with 1 mL of equilibration buffer and enzyme was  
16 stored at 4 °C until further use. The protein concentration was determined with the Bio-  
17 Rad Protein Assay (Bio-Rad, Hercules, CA, USA) based on the Bradford method [25],  
18 using bovine serum albumin as a protein standard.

19 LPMO reaction mixtures contained 5 g/L of phosphoric acid-swollen cellulose (PASC),  
20 1 μM *TaAA9A*, 1 mM ascorbic acid (AscA) or 10 g/L of SSL as a reductant, and 50  
21 mM sodium acetate pH 5.0. PASC was prepared from Avicel according to a previously  
22 described procedure [26]. Reactions were carried out in 2 mL reaction tubes with 200  
23 μL total reaction volume incubated at 50 °C for 24 h, in a ThermoMixer (Eppendorf,

1 Hamburg, Germany) with orbital shaking at 750 rpm. Reactions were terminated by  
2 filtration in 96-well plates with 0.45 µm PES filter (Merck Millipore, Billerica, MA,  
3 USA). Supernatants were stored at -20 °C until further analysis. Control experiments  
4 were performed in the absence of either reductant or enzyme.

### 5 **2.3. Enzymatic hydrolysis in bioreactors**

6 The mass of the hydrolysis reaction was 1.0 kg, containing 120 g pretreated spruce  
7 solids (12% DM) and the rest (880 g) was defined as hydrolysis liquid. In all hydrolysis  
8 reactions, SSL was used as the reductant. In standard reactions, SSL was mixed with  
9 water and pretreated spruce solids to reach a final concentration of 10 g SSL DM per  
10 liter hydrolysis liquid.

11 The hydrolysis experiments were carried out in Biostat A Plus bioreactors (Sartorius,  
12 Melsungen, Germany). The reactor vessel with a diameter of 130 mm was equipped  
13 with a 70 mm diameter pitched-blade impeller. The impeller speed was maintained at  
14 300 rpm. The solids were fed gradually to the reactor during the first 30 min of the  
15 hydrolysis reaction to improve initial mixing. All hydrolysis reactions were run for 72 h,  
16 and in some cases, the reaction time was prolonged to 144 h.

17 The enzyme preparation used (Cellic CTec3) was kindly provided by Novozymes A/S  
18 (Bagsvaerd, Denmark). The enzyme loading used was 0.04 g enzyme solution/g  
19 pretreated spruce solids (based on DM). The temperature was maintained at 50 °C in all  
20 experiments. The pH was maintained at 5.0 by controlled addition of 3 M NaOH. To  
21 create consistent aerobic or anaerobic conditions the hydrolysis liquid was sparged  
22 before the start of hydrolysis with either 200 mL/min air or nitrogen gas. To maintain  
23 aerobic or anaerobic conditions during hydrolysis the headspace was flushed with either

1 200 mL/min air or nitrogen gas. In this study concentrations of dissolved O<sub>2</sub> (DO) lower  
2 than 0.1% were considered as anaerobic conditions. However, even DO lower than  
3 0.1% may affect oxidation-reduction potential (ORP) measurements.

4 In constant feed experiments H<sub>2</sub>O<sub>2</sub> (0.5 wt%) was fed to the reactor at a feed rate of 1.2  
5 mL/h using a Watson-Marlow 120 peristaltic pump (Watson-Marlow, Falmouth,  
6 Cornwall, England). This corresponds to a feed rate of 200 μmol/h of H<sub>2</sub>O<sub>2</sub> per liter of  
7 hydrolysis liquid. The feed of H<sub>2</sub>O<sub>2</sub> was started 16 hours after the start of hydrolysis in  
8 order to allow time for viscosity reduction and improve mixing. The 95% mixing time,  
9 i.e. the time for a normalized probe signal to reach and remain within 100±5% of the  
10 final value after a perturbation, was determined to be less than 10 seconds at the onset  
11 of H<sub>2</sub>O<sub>2</sub> feeding, indicating that local accumulation of H<sub>2</sub>O<sub>2</sub> can be neglected. In control  
12 experiments with no H<sub>2</sub>O<sub>2</sub> feed, H<sub>2</sub>O was fed instead at a feed rate of 1.2 mL/h.

#### 13 **2.4. Oxidation-reduction potential (ORP) measurement**

14 The ORP was measured with a combination redox electrode (Pt4805-DPAS-SC-  
15 K8S/200, Mettler-Toledo, Greifensee, Switzerland) consisting of a Pt electrode and a  
16 reference equivalent to Ag / AgCl / 3 M KCl. The redox electrode was connected to a  
17 transmitter (Multi-parameter Transmitter M300, Mettler-Toledo, Greifensee,  
18 Switzerland) that provided the voltage reading. ORP is shown relative to the reference  
19 electrode; ORP relative to the standard hydrogen electrode (SHE) can be calculated  
20 according to:  $ORP_{SHE} = ORP + 187.6 \text{ mV}$ .

21 For ORP controlled enzymatic hydrolysis experiments a feed-back regulated on/off  
22 control of ORP was implemented. In short, a 4 mV ORP dead-band was applied around  
23 the ORP set-point (± 2 mV), and if the ORP decreased below this value feeding of H<sub>2</sub>O<sub>2</sub>



1 (0.5 wt%) at a feed rate of 6 mL/h was initiated until the ORP increased above this  
2 value.

### 3 **2.5. Analysis of monosaccharides and C4-oxidized dimer**

4 Samples of the hydrolysis liquid in 2 mL Eppendorf tubes were separated by  
5 centrifugation at  $14850 \times g$  for 5 min. The supernatant was filtered through 0.2  $\mu\text{m}$   
6 filters. The samples were then heated in a water bath for 10 min at 100 °C to inactivate  
7 the enzymes. Following inactivation, the samples were cooled on ice and stored at -20  
8 °C until analysis. Concentrations of monomeric sugars were measured by HPLC (high-  
9 performance liquid chromatography). In short, the sugars were separated on a polymer  
10 column (Aminex HPX-87P, Bio-Rad Laboratories, München, Germany) at 85 °C.  
11 Deionized water (Purelab Flex, Elga, Marlow, UK) was used as eluent at a flow rate of  
12 0.6 mL/min. The sugars were detected with a refractive index detector (Waters 2410,  
13 Waters, Milford, MA, USA).

14 Glucan conversion, i.e. the percent of glucan converted to glucose, was calculated as  
15 follows. The density of the hydrolysis liquid ( $\rho$ ) was calculated based on the measured  
16 concentrations of glucose ( $c_{\text{Glc}}$ ), mannose ( $c_{\text{Man}}$ ) and xylose ( $c_{\text{Xyl}}$ ) only, as the  
17 concentrations of other sugars were negligible [27]:

$$18 \quad \rho = 1000 + 0.35(c_{\text{Glc}} + c_{\text{Man}} + c_{\text{Xyl}})$$

19 The volume of the hydrolysis liquid ( $V$ ) was solved from a mass balance based on the  
20 initial mass of hydrolysis liquid ( $m_0 = 880 \text{ g}$ ), the mass added with the  $\text{H}_2\text{O}_2$  feed  
21 ( $m_{\text{feed}}$ ), the mass of monosaccharides released by hydrolysis ( $m_{\text{hyd sug}}$ ) and the mass of  
22 water taken up during hydrolysis ( $m_{\text{hyd H}_2\text{O}}$ ):

$$23 \quad \rho V = m_0 + m_{\text{feed}} + m_{\text{hyd sug}} - m_{\text{hyd H}_2\text{O}}$$

1 
$$m_{\text{hyd sug}} = (c_{\text{Glc}} + c_{\text{Man}} + c_{\text{Xyl}})V - (c_{\text{Glc0}} + c_{\text{Man0}} + c_{\text{Xyl0}})V_0$$

2 
$$m_{\text{hyd H}_2\text{O}} = 0.1[(c_{\text{Glc}} + c_{\text{Man}})V - (c_{\text{Glc0}} + c_{\text{Man0}})V_0] + 0.12[c_{\text{Xyl}}V - c_{\text{Xyl0}}V_0]$$

3 Finally, the glucan conversion (C) was calculated based on the mass of glucose released  
4 by hydrolysis, initial mass of pretreated spruce solids ( $m_{s0} = 120$  g) and the initial  
5 glucan fraction in the solids ( $\chi_0 = 0.874$ ), according to:

6 
$$C = 100 \frac{c_{\text{Glc}}V - c_{\text{Glc0}}V_0}{1.111\chi_0 m_{s0}}$$

7 LPMOs acting on cellulose may oxidize the C1 or the C4 position in the scissile  
8 glycosidic bond, whereas some LPMOs generate mixtures of C1- and C4- oxidized  
9 products [12,28]. In the presence of cellulase and  $\beta$ -glucosidase activity, as is the case  
10 with commercial cellulase cocktails, two soluble oxidized products are formed: the C1-  
11 oxidized monomer, i.e. gluconic acid, and the C4-oxidized dimer, i.e. Glc4gemGlc. The  
12 type and amount of LPMOs present in Cellic CTec3 is unknown. Under our reaction  
13 conditions Glc4gemGlc was the main product. Due to the high signal background,  
14 adversely affecting the analysis of gluconic acid, only Glc4gemGlc was analyzed in the  
15 study, as a proxy of LPMO activity. Importantly, there are difficulties with analysis of  
16 Glc4gemGlc, as it is unstable, particularly at high pH, meaning that it decomposes  
17 during the reaction, sample processing, and on the column during product analysis  
18 [13,29]. These issues were minimized by keeping the standard and the samples in the  
19 same conditions during sample processing and analysis. Nonetheless, the measured  
20 values should serve more as indications of trends rather than absolute values. Overall,  
21 the amounts of detected C4-oxidized products never exceeded 0.8% of the total amount  
22 of glucan  $\beta$ -1,4 linkages in the reaction mixture.

1 Concentrations of the C4-oxidized dimer (Glc4gemGlc) were analyzed with HPAEC-  
2 PAD (high-performance anion exchange chromatography with pulsed amperometric  
3 detection) using a Dionex ICS 5000 system (Dionex, Sunnyvale, CA, USA) equipped  
4 with a CarboPac PA1 4×250 mm analytical column and a CarboPac PA1 4×50 mm  
5 guard column operating at an eluent flow rate of 1 mL/min [9,30]. In short, initial  
6 conditions were set to 0.1 M NaOH (100% eluent A), followed by a linear gradient  
7 towards increasing concentrations of eluent B (1 M sodium acetate in 0.1 M NaOH),  
8 reaching 10% B 10 min after sample injection and 30% B at 35 min after injection. This  
9 was followed by a 5 min exponential gradient to 100% eluent B, after which the column  
10 was reconditioned by running the initial conditions for 9 min. C4-oxidized standards  
11 were generated by degrading cellopentaose with *NcLPMO9C* [9].

### 12 **3. Results and discussion**

#### 13 **3.1. SSL as reductant for LPMOs**

14 Comparing product formation by *TaAA9A* in reactions with PASC using either 1 mM  
15 AscA or 10 g/L of SSL showed no difference in released oxidized sugars (Fig. 1),  
16 indicating that SSL is capable to reduce LPMOs and drive the oxidative cleavage of  
17 insoluble cellulosic substrate. It had been shown previously that lignosulfonates, which  
18 are derived from SSL by fermentation and subsequent evaporation, can activate the  
19 LPMO-containing Cellic CTec3 preparation releasing oxidized sugars during aerobic  
20 hydrolysis of sulfite-pulped Norway spruce [23]. It is interesting to note that the release  
21 of oxidized sugars from PASC, which is nearly devoid of lignin, suggests that SSL is  
22 able to drive the LPMO reaction without the need of solid lignin bound to the substrate.  
23 It is plausible that the interplay between sulfonated lignin fractions of different

1 molecular weight, analogous to the interplay between low and high molecular lignin  
2 fractions [7], enables LPMO reduction by the SSL.

### 3 **3.2. Monitoring ORP during enzymatic hydrolysis**

4 In this study, we used a platinum electrode for monitoring the ORP during enzymatic  
5 hydrolysis reactions in laboratory bioreactors under conditions similar to those expected  
6 in industrial processing. As previously mentioned,  $O_2$  and  $H_2O_2$  are both possible co-  
7 substrates for the LPMO catalyzed oxidation of cellulose. The ORP measured by a  
8 platinum electrode is affected by the concentration of dissolved  $O_2$  (DO) and  $H_2O_2$   
9 during enzymatic hydrolysis, and the electrode signal may therefore provide useful  
10 information on the redox state of the solution, which likely affects the capacity for  
11 LPMO reactions to take place. It is, however, important to keep in mind that the  
12 measured ORP may not depend directly on the concentration of  $H_2O_2$ , but may reflect  
13 changes in the ratio of other redox couples present in the system [31].

14 In a series of initial experiments, the ORP was measured for enzymatic hydrolysis  
15 reactions under aerobic and anaerobic conditions, and with and without  $H_2O_2$  feeding  
16 ( $200 \mu\text{mol/Lh}$  starting at 16 h). The enzymatic hydrolysis reaction under anaerobic  
17 conditions without  $H_2O_2$  feeding represented a control experiment without LPMO  
18 catalyzed oxidation. Glucan conversion during the initial phase of hydrolysis was  
19 similar in all experiments (Fig. 2A). In the reactions without addition of  $H_2O_2$ , the  
20 curves started to diverge after 16 hours, showing more rapid hydrolysis under aerobic  
21 conditions. The higher efficiency of the aerobic reaction was expected since Cellic  
22 CTec3 contains LPMOs whose activity is affected by oxygen and similar observations  
23 have been made before [23].  $H_2O_2$  feeding starting at 16 hours significantly increased  
24 the hydrolysis rate in both aerobic and anaerobic conditions. Importantly, this higher

1 hydrolysis rate was not sustained during the last 24 hours of the reaction carried out  
2 under aerobic conditions.

3 Measurements of the levels of C4-oxidized dimers (Glc4gemGlc) showed interesting  
4 correlations between LPMO activity and glucan conversion (Fig. 2B). In agreement  
5 with previous reports on sulfite pretreated spruce [13], there was no Glc4gemGlc  
6 production under anaerobic conditions in the absence of H<sub>2</sub>O<sub>2</sub> (i.e. condition that gave  
7 the lowest glucose yields; Fig. 2A). During aerobic hydrolysis without added H<sub>2</sub>O<sub>2</sub> the  
8 production of Glc4gemGlc was slow and steady, likely driven by H<sub>2</sub>O<sub>2</sub> generated from  
9 dissolved oxygen and reducing agents in the spent sulfite liquor (SSL). Feeding of H<sub>2</sub>O<sub>2</sub>  
10 led to a drastic increase in the rate of Glc4gemGlc production (and an increase in  
11 glucose yields; Fig. 2A). In the aerobic reaction with H<sub>2</sub>O<sub>2</sub> feed, the rate of Glc4gemGlc  
12 production started decreasing in the period around 48 hours, soon after which the levels  
13 of Glc4gemGlc started decreasing due to the instability of this compound [13]. The stop  
14 in Glc4gemGlc production coincided with a decrease in the enzymatic hydrolysis rate  
15 (Fig. 2A). Interestingly, LPMO activity lasted longer under anaerobic conditions (Fig.  
16 2B), and this was reflected in a higher glucose release rate in the final phase of the  
17 reaction (Fig. 2A). The levels of Glc4gemGlc in the anaerobic reaction started  
18 decreasing after the 72 hour time-point due to the instability of C4-oxidized dimer  
19 (Suppl. fig. 1).

20 It seems that, with this H<sub>2</sub>O<sub>2</sub> feeding rate, oxidative inactivation of LPMO is promoted  
21 by the presence of oxygen, possibly because overall H<sub>2</sub>O<sub>2</sub> levels are higher due to  
22 reactions between O<sub>2</sub> and reducing compounds (likely including reduced LPMOs) in the  
23 hydrolysis mixture [32]. Overall, the results depicted in Figs. 2A & 2B support the

1 importance of LPMO activity for the overall hydrolysis rate, particularly in the late  
2 phases of the hydrolysis reaction.

3 Fig. 2C shows that, as expected, the ORP was higher under aerobic compared to  
4 anaerobic conditions. In the absence of H<sub>2</sub>O<sub>2</sub> feeding, the ORP increased very slowly  
5 during the aerobic hydrolysis and was essentially constant. With H<sub>2</sub>O<sub>2</sub> feeding, the ORP  
6 initially had a similar profile, but it started increasing rapidly in the period around 48  
7 hours, coinciding with the loss of LPMO activity visible in Fig. 2B. Fig. 2C further  
8 shows that in anaerobic hydrolysis without H<sub>2</sub>O<sub>2</sub> feed, the ORP decreased during the  
9 initial phase of the reaction. At the start of H<sub>2</sub>O<sub>2</sub> feeding in anaerobic conditions the  
10 ORP increased rapidly, after which it stabilized at a relatively constant level. In the  
11 period around 48 hours the ORP started increasing again, and this coincided with the  
12 reduced LPMO activity (Fig. 2B).

13 The initial decrease in ORP during anaerobic hydrolysis without H<sub>2</sub>O<sub>2</sub> feed was most  
14 likely caused by gradual removal of remaining dissolved oxygen (DO). Schuldiner et al.  
15 observed a decrease in ORP of 59.1 mV for a 10-fold decrease in DO, by measuring the  
16 potential of a platinum electrode immersed in a solution of 1 M H<sub>2</sub>SO<sub>4</sub> at 25 °C, while  
17 varying the partial pressure of oxygen in the range of 10<sup>-6</sup> to 10<sup>-2</sup> atm [33]. The low  
18 ORP in the anaerobic hydrolysis reactions may promote the reduction of LPMOs, as the  
19 formal potentials of LPMOs vs Ag/AgCl (45 mV for *ScAA10C* and 54 mV for  
20 *ScAA10B* [34]; -42 mV for *PaAA9E* and 129 mV for *PaAA9H* [35]; -2 mV for  
21 *TaAA9A* [36]; 80 mV for *FoAA9* and 125 mV for *MtAA9* [37]) are in most cases much  
22 higher.

23 Fig. 2C shows that an increase in ORP occurs *during H<sub>2</sub>O<sub>2</sub> feeding* in three different  
24 cases: (1) aerobic hydrolysis when the LPMO activity starts to decrease, (2) anaerobic

1 hydrolysis at the start of H<sub>2</sub>O<sub>2</sub> feeding, and (3) anaerobic hydrolysis when the LPMO  
2 activity starts to decrease. Control experiments without added enzyme showed that the  
3 ORP increases directly at the start of H<sub>2</sub>O<sub>2</sub> feeding in both aerobic and anaerobic  
4 conditions, and continues to increase during feeding (Suppl. fig. 2). One could envisage  
5 that the three cases of ORP increase shown in Fig. 2C are due to: (1) and (3) a  
6 slowdown and eventual termination of LPMO activity, meaning that added H<sub>2</sub>O<sub>2</sub> is no  
7 longer consumed and is accumulating, and (2) a short period of H<sub>2</sub>O<sub>2</sub> “overshoot”  
8 directly after initiation of H<sub>2</sub>O<sub>2</sub> feeding, before a steady-state is reached.

### 9 **3.3. ORP controlled feeding of H<sub>2</sub>O<sub>2</sub>**

10 Since LPMO activity apparently is connected to the ORP value, it was of interest to  
11 investigate the possibility of controlling the feed rate of H<sub>2</sub>O<sub>2</sub> based on the ORP. The  
12 feed rate was therefore manipulated to keep the ORP value at different set-points using  
13 a simple dead-band feed-back control. In this way, the effect of the different set-points  
14 on the LPMO catalyzed oxidation could be assessed.

15 In anaerobic reactions, the ORP was kept at -120 mV, -80 mV or -40 mV, i.e. above the  
16 low ORP plateau of -180 mV that was reached during anaerobic hydrolysis with no  
17 feeding (Fig. 2C). In aerobic conditions the range of feasible ORP set-points was more  
18 limited due to the large effect of oxygen on the ORP signal. ORP control was started  
19 after 2 hours (ORP at 110 mV) or after 42 hours (ORP at 120 mV). These ORP set-  
20 points were slightly higher than the ORP measured for aerobic hydrolysis without H<sub>2</sub>O<sub>2</sub>  
21 feed (Fig. 2C). As the ORP increases gradually during enzymatic hydrolysis in aerobic  
22 conditions making it difficult to maintain an ORP set-point during the whole reaction,  
23 an additional experiment was performed during which the ORP was controlled  
24 according to a linear profile between 110 mV at 2 hours and 150 mV at 72 hours.

1 In the anaerobic reactions, the initial rate of enzymatic hydrolysis (0 to 24 h) was  
2 higher, the higher the ORP set-point (Fig. 3A). However, control at the highest ORP (-  
3 40 mV), which implies the largest amount of added H<sub>2</sub>O<sub>2</sub>, led to early enzyme  
4 inactivation, as observed by a reduced hydrolysis rate and cessation of LPMO activity  
5 (Figs. 3A,B). Control at -80 mV led to a maintained hydrolysis rate throughout the  
6 complete incubation period and a higher final glucose yield. Maintaining the ORP at  
7 even lower level (-120 mV) led to slower hydrolysis when compared to control at -80  
8 mV.

9 The rate of Glc4gemGlc production was higher, the higher the ORP set-points (Fig.  
10 3B), which was likely due to higher resulting H<sub>2</sub>O<sub>2</sub> feed rates (Fig. 3D). Compared to  
11 the -40 mV reaction, controlling the ORP at a lower level (-80 mV) led to a prolonged  
12 period of LPMO-catalyzed oxidation. The prolonged LPMO activity was reflected in  
13 higher final glucan conversion (Fig. 3A). Higher LPMO reaction rates were  
14 accompanied by an earlier stop in Glc4gemGlc production. The -40 mV LPMO reaction  
15 stopped within the first 48 hours (Fig. 3B), while the -80 mV reaction stopped after the  
16 72 hour time-point and the -120 mV reaction was maintained for 144 hours (Suppl. fig.  
17 1). Fig. 3C shows the measured ORP during the ORP controlled anaerobic reactions; the  
18 feeding started later at lower ORP set-points as it took more time to reach these lower  
19 ORP values during hydrolysis (Fig. 3D).

20 The two ORP set-point control experiments performed in aerobic conditions showed  
21 clear differences (Fig. 4). When starting the control at 2 hours (110 mV), the initial rate  
22 of enzymatic hydrolysis (0 to 24 h) was slightly higher (Fig. 4A). However, this set-up  
23 caused an early stop in Glc4gemGlc production (Fig. 4B), with a concomitant decrease  
24 in enzymatic hydrolysis rate in the later stages of the reaction and decreased final



1 glucose yields. In contrast, starting the ORP control and H<sub>2</sub>O<sub>2</sub> feeding at 42 hours (120  
2 mV) allowed the reaction to reach a higher glucan conversion after 72 hours (72%). In  
3 this case the stop in LPMO activity occurred after the 72 hour time-point (Suppl. Fig.  
4 1). The ORP control ramp experiment (110 to 150 mV) gave overall very similar results  
5 to the ORP set-point control experiment starting at 2 hours (Fig. 4).

### 6 **3.4. Loss of LPMO activity or lack of electron donor?**

7 The seemingly abrupt stop in LPMO activity in certain hydrolysis reactions with H<sub>2</sub>O<sub>2</sub>  
8 feeding (e.g. Fig. 2B) is an interesting phenomenon. This was first reported by Müller et  
9 al. who suggested that inactivation is caused by high feed rates of H<sub>2</sub>O<sub>2</sub>, which would  
10 lead to LPMO self-inactivation in situations where the LPMO substrate becomes  
11 depleted [13]. Although a more fundamental inquiry into this phenomenon was outside  
12 the scope of the present study, a set of hydrolysis experiments were performed to  
13 explore the phenomenon: (1) hydrolysis with a double dose of added SSL, thus  
14 containing a double initial dose of the electron donor, (2) hydrolysis with an ORP-  
15 controlled feed of SSL, thus preventing the electron donor to be exhausted from the  
16 medium during the hydrolysis, (3) hydrolysis with a second dose of enzyme added close  
17 to the time-point (42 h) when the LPMO activity starts decreasing in aerobic reactions  
18 with H<sub>2</sub>O<sub>2</sub> feeding. The experiments were performed under aerobic conditions with a  
19 constant H<sub>2</sub>O<sub>2</sub> feed of 200 µmol/Lh.

20 Use of a double dose of SSL or ORP-controlled feeding of SSL had little effect on  
21 glucan conversion (Fig. 5A), which was similar to the results from the baseline aerobic  
22 H<sub>2</sub>O<sub>2</sub> feeding case (Fig. 2A). Addition of a 2<sup>nd</sup> dose of CTec3 at 42 hours significantly  
23 increased the glucan conversion and the reaction reached almost full conversion after 72  
24 hours. Neither a double initial dose of SSL nor controlled SSL feeding extended the

1 period of Glc4gemGlc production, indicating that the stop in LPMO activity was not  
2 caused by a lack of electron donor (Fig. 5B). Addition of a second dose of CTec3 at 42  
3 hours prolonged Glc4gemGlc production, indicating that fresh LPMOs - but not more  
4 electron donors - were needed to continue the reaction.

5 Enzymatic hydrolysis with a double dose of SSL underwent a rapid increase in ORP  
6 associated with a stop in Glc4gemGlc production (Fig. 5C), very similar to the baseline  
7 aerobic H<sub>2</sub>O<sub>2</sub> feeding case (Fig. 2C). ORP-controlled addition of SSL prevented this  
8 increase in ORP and kept it constant at 110 mV, likely because H<sub>2</sub>O<sub>2</sub> that would  
9 otherwise accumulate due to the cessation of LPMO activity reacts with the added  
10 reductant in SSL. The second addition of CTec3 at 42 hours delayed the increase in  
11 ORP to around 60 hours, indicating that the addition of fresh LPMO extended the  
12 enzymatic consumption of H<sub>2</sub>O<sub>2</sub>. In this latter case, the ORP started increasing as  
13 glucan conversion approached 100%, meaning that there would be hardly any LPMO  
14 substrate left.

#### 15 **4. Conclusions**

16 The present results show that ORP is a useful on-line measurement tool, which can also  
17 be used for feed-back control of hydrogen peroxide addition. The precision is better and  
18 the span of control set-points is greater for anaerobic conditions, since the redox signal  
19 is not affected (“polluted”) by oxygen from the air. The oxidative damage of LPMOs  
20 can therefore likely be better controlled under anaerobic conditions with hydrogen  
21 peroxide addition. However, there is no reason to believe that a fixed set-point  
22 represents a global optimum. We believe that further optimization should be possible,  
23 perhaps fueled by growing insight into the determinants of LPMO stability, and of the  
24 interplay between LPMOs and other enzymes in the cellulase cocktail.

## 1 **References**

- 2 [1] G. Vaaje-Kolstad, B. Westereng, S.J. Horn, Z. Liu, H. Zhai, M. Sørlie, V.G.H. Eijsink,  
3 An oxidative enzyme boosting the enzymatic conversion of recalcitrant polysaccharides,  
4 *Science*. 330 (2010) 219–222. doi:10.1126/science.1192231.
- 5 [2] J.A. Langston, T. Shaghasi, E. Abbate, F. Xu, E. Vlasenko, M.D. Sweeney,  
6 Oxidoreductive cellulose depolymerization by the enzymes cellobiose dehydrogenase and  
7 glycoside hydrolase 61, *Appl. Environ. Microbiol.* 77 (2011) 7007–7015.  
8 doi:10.1128/AEM.05815-11.
- 9 [3] R.J. Quinlan, M.D. Sweeney, L. Lo Leggio, H. Otten, J.-C.N. Poulsen, K.S. Johansen,  
10 K.B.R.M. Krogh, C.I. Jorgensen, M. Tovborg, A. Anthonsen, T. Tryfona, C.P. Walter, P.  
11 Dupree, F. Xu, G.J. Davies, P.H. Walton, Insights into the oxidative degradation of cellulose by  
12 a copper metalloenzyme that exploits biomass components, *Proc. Natl. Acad. Sci.* 108 (2011)  
13 15079–15084. doi:10.1073/pnas.1105776108.
- 14 [4] C.M. Phillips, W.T. Beeson, J.H. Cate, M.A. Marletta, Cellobiose dehydrogenase and a  
15 copper-dependent polysaccharide monooxygenase potentiate cellulose degradation by  
16 *Neurospora crassa*, *ACS Chem. Biol.* 6 (2011) 1399–1406. doi:10.1021/cb200351.
- 17 [5] Z. Forsberg, G. Vaaje-Kolstad, B. Westereng, A.C. Bunsæ, Y. Stenstrøm, A.  
18 Mackenzie, M. Sørlie, S.J. Horn, V.G.H. Eijsink, Cleavage of cellulose by a cbm33 protein,  
19 *Protein Sci.* 20 (2011) 1479–1483. doi:10.1002/pro.689.
- 20 [6] J. Hu, V. Arantes, A. Pribowo, J.N. Saddler, The synergistic action of accessory  
21 enzymes enhances the hydrolytic potential of a “cellulase mixture” but is highly substrate  
22 specific, *Biotechnol. Biofuels.* 6 (2013) 1–12. doi:10.1186/1754-6834-6-112.
- 23 [7] B. Westereng, D. Cannella, J. Wittrup Agger, H. Jørgensen, M. Larsen Andersen,  
24 V.G.H. Eijsink, C. Felby, Enzymatic cellulose oxidation is linked to lignin by long-range  
25 electron transfer, *Sci. Rep.* 5 (2015) 1–9. doi:10.1038/srep18561.

- 1 [8] D. Cannella, C.C. Hsieh, C. Felby, H. Jørgensen, Production and effects of aldonic acids  
2 during enzymatic hydrolysis of lignocelluloses at high dry matter content, *Biotechnol Biofuels*.  
3 5 (2012) 1–10. doi:10.1186/1754-6834-5-26.
- 4 [9] G. Müller, A. Várnai, K.S. Johansen, V.G.H. Eijsink, S.J. Horn, Harnessing the  
5 potential of LPMO-containing cellulase cocktails poses new demands on processing conditions,  
6 *Biotechnol. Biofuels*. 8 (2015) 187. doi:10.1186/s13068-015-0376-y.
- 7 [10] D. Cannella, H. Jørgensen, Do new cellulolytic enzyme preparations affect the  
8 industrial strategies for high solids lignocellulosic ethanol production?, *Biotechnol. Bioeng.* 111  
9 (2014) 59–68. doi:10.1002/bit.25098.
- 10 [11] B. Bissaro, Å.K. Røhr, G. Müller, P. Chylenski, M. Skaugen, Z. Forsberg, S.J. Horn, G.  
11 Vaaje-Kolstad, V.G.H. Eijsink, Oxidative cleavage of polysaccharides by monocopper enzymes  
12 depends on H<sub>2</sub>O<sub>2</sub>, *Nat. Chem. Biol.* 13 (2017) 1123–1128. doi:10.1038/nchembio.2470.
- 13 [12] T. Isaksen, B. Westereng, F.L. Aachmann, J. Wittrup Agger, D. Kracher, R. Kittl, R.  
14 Ludwig, D. Haltrich, V.G.H. Eijsink, S.J. Horn, A C<sub>4</sub>-oxidizing lytic polysaccharide  
15 monooxygenase cleaving both cellulose and cello-oligosaccharides, *J. Biol. Chem.* 289 (2014)  
16 2632–2642. doi:10.1074/jbc.M113.530196.
- 17 [13] G. Müller, P. Chylenski, B. Bissaro, V.G.H. Eijsink, S.J. Horn, The impact of hydrogen  
18 peroxide supply on LPMO activity and overall saccharification efficiency of a commercial  
19 cellulase cocktail, *Biotechnol. Biofuels*. 11 (2018) 1–17. doi:10.1186/s13068-018-1199-4.
- 20 [14] B.R. Scott, H.Z. Huang, J. Frickman, R. Halvorsen, K.S. Johansen, Catalase improves  
21 saccharification of lignocellulose by reducing lytic polysaccharide monooxygenase-associated  
22 enzyme inactivation, *Biotechnol. Lett.* 38 (2016) 425–434. doi:10.1007/s10529-015-1989-8.
- 23 [15] S. Kuusk, B. Bissaro, P. Kuusk, Z. Forsberg, V.G.H. Eijsink, M. Sørli, P. Väljamäe,  
24 Kinetics of H<sub>2</sub>O<sub>2</sub>-driven degradation of chitin by a bacterial lytic polysaccharide  
25 monooxygenase, *J. Biol. Chem.* 293 (2018) 523–531. doi:10.1074/jbc.M117.817593.

- 1 [16] J.O. Bockris, A.K.N. Reddy, M. Gamboa-Aldeco, Modern Electrochemistry 2A  
2 Fundamentals of Electrode Processes, 2<sup>nd</sup> ed., Springer, Boston, MA, 2000.
- 3 [17] F.A. Koch, W.K. Oldham, Oxidation-reduction potential - A tool for monitoring,  
4 control and optimization of biological nutrient removal systems, Water Sci. Technol. 17 (1985)  
5 259–281. doi:10.2166/wst.1985.0237.
- 6 [18] Y.-O. Kim, H.-U. Nam, Y.-R. Park, J.-H. Lee, T.-J. Park, T.-H. Lee, Fenton oxidation  
7 process control using oxidation-reduction potential measurement for pigment wastewater  
8 treatment, Korean J. Chem. Eng. 21 (2004) 801–805. doi:10.1007/BF02705523.
- 9 [19] A. Ishizaki, H. Shibai, Y. Hirose, Basic aspects of electrode potential change in  
10 submerged fermentation, Agric. Biol. Chem. 38 (1974) 2399–2406.  
11 doi:10.1080/00021369.1974.10861537.
- 12 [20] C.G. Liu, C. Xue, Y.H. Lin, F.W. Bai, Redox potential control and applications in  
13 microaerobic and anaerobic fermentations, Biotechnol. Adv. 31 (2013) 257–265.  
14 doi:10.1016/j.biotechadv.2012.11.005.
- 15 [21] A. Sluiter, B. Hames, R. Ruiz, C. Scarlata, J. Sluiter, D. Templeton, Determination of  
16 Sugars, Byproducts, and Degradation Products in Liquid Fraction Process Samples, NREL,  
17 Golden, CO, 2008.
- 18 [22] A. Sluiter, B. Hames, R. Ruiz, C. Scarlata, J. Sluiter, D. Templeton, D. Crocker,  
19 Determination of Structural Carbohydrates and Lignin in Biomass, NREL, Golden, CO, 2008.
- 20 [23] P. Chylenski, D.M. Petrović, G. Müller, M. Dahlström, O. Bengtsson, M. Lersch, M.  
21 Siika-Aho, S.J. Horn, V.G.H. Eijsink, Enzymatic degradation of sulfite-pulped softwoods and  
22 the role of LPMOs, Biotechnol. Biofuels. 10 (2017) 1–13. doi:10.1186/s13068-017-0862-5.
- 23 [24] J.S. Loose, Z. Forsberg, M.W. Fraaije, V.G. Eijsink, G. Vaaje-Kolstad, A rapid  
24 quantitative activity assay shows that the *Vibrio cholerae* colonization factor GbpA is an active

1 lytic polysaccharide monooxygenase, *FEBS Lett.* 588 (2014) 3435–3440.  
2 doi:10.1016/j.febslet.2014.07.036.

3 [25] M.M. Bradford, A rapid and sensitive method for the quantitation of microgram  
4 quantities of protein utilizing the principle of protein-dye binding., *Anal. Biochem.* 72 (1976)  
5 248–54. doi:10.1016/0003-2697(76)90527-3.

6 [26] T.M. Wood, Preparation of crystalline, amorphous, and dyed cellulase substrates.,  
7 *Methods Enzymol.* 160 (1988) 19–25. doi:10.1016/0076-6879(88)60103-0.

8 [27] Y. Zhu, M. Malten, M. Torry-Smith, J.D. McMillan, J.J. Stickel, Calculating sugar  
9 yields in high solids hydrolysis of biomass., *Bioresour. Technol.* 102 (2011) 2897–2903.  
10 doi:10.1016/j.biortech.2010.10.134.

11 [28] V.V. Vu, W.T. Beeson, C.M. Phillips, J.H. Cate, M.A. Marletta, Determinants of  
12 regioselective hydroxylation in the fungal polysaccharide monooxygenases., *J. Am. Chem. Soc.*  
13 136 (2014) 562–565. doi:10.1021/ja409384b.

14 [29] B. Westereng, M.O. Arntzen, F.L. Aachmann, A. Várnai, V.G.H. Eijsink, J.W. Agger,  
15 Simultaneous analysis of C1 and C4 oxidized oligosaccharides, the products of lytic  
16 polysaccharide monooxygenases acting on cellulose., *J. Chromatogr. A.* 1445 (2014) 46–54.  
17 doi:10.1016/j.chroma.2016.03.064.

18 [30] B. Westereng, J. Wittrup Agger, S.J. Horn, G. Vaaje-Kolstad, F.L. Aachmann, Y.H.  
19 Stenstrøm, V.G.H. Eijsink, Efficient separation of oxidized cello-oligosaccharides generated by  
20 cellulose degrading lytic polysaccharide monooxygenases, *J. Chromatogr. A.* 1271 (2013) 144–  
21 152. doi:10.1016/j.chroma.2012.11.048.

22 [31] J.O. Bockris, L.F. Oldfield, The oxidation-reduction reactions of hydrogen peroxide at  
23 inert metal electrodes and mercury cathodes, *Trans. Faraday Soc.* 51 (1955) 249–259.  
24 doi:10.1039/TF9555100249.

- 1 [32] V.G.H. Eijsink, D. Petrović, Z. Forsberg, S. Mekasha, Å.K. Røhr, A. Várnai, B.  
2 Bissaro, G. Vaaje-Kolstad, On the functional characterization of lytic polysaccharide  
3 monoxygenases (LPMOs), *Biotechnol. Biofuels.* 12 (2019) 1–16. doi:10.1186/s13068-019-  
4 1392-0.
- 5 [33] S. Schuldiner, B.J. Piersma, T.B. Warner, Potential of a platinum electrode at low  
6 partial pressures of hydrogen and oxygen II. An improved gas-tight system with a negligible  
7 oxygen leak, *J. Electrochem. Soc.* 113 (1966) 573–577. doi:10.1149/1.2424029.
- 8 [34] Z. Forsberg, A.K. Mackenzie, M. Sorlie, A.K. Røhr, R. Helland, A.S. Arvai, G. Vaaje-  
9 Kolstad, V.G.H. Eijsink, Structural and functional characterization of a conserved pair of  
10 bacterial cellulose-oxidizing lytic polysaccharide monoxygenases, *Proc. Natl. Acad. Sci.* 111  
11 (2014) 8446–8451. doi:10.1073/pnas.1402771111.
- 12 [35] S. Garajova, Y. Mathieu, M.R. Beccia, C. Bennati-Granier, F. Biaso, M. Fanuel, D.  
13 Ropartz, B. Guigliarelli, E. Record, H. Rogniaux, B. Henrissat, J.G. Berrin, Single-domain  
14 flavoenzymes trigger lytic polysaccharide monoxygenases for oxidative degradation of  
15 cellulose, *Sci. Rep.* 6 (2016) 1–9. doi:10.1038/srep28276.
- 16 [36] D.M. Petrović, B. Bissaro, P. Chylenski, M. Skaugen, M. Sørlie, M.S. Jensen, F.L.  
17 Aachmann, G. Courtade, A. Várnai, V.G.H. Eijsink, Methylation of the N-terminal histidine  
18 protects a lytic polysaccharide monoxygenase from auto-oxidative inactivation, *Protein Sci.* 27  
19 (2018) 1636–1650. doi:10.1002/pro.3451.
- 20 [37] D. Zouraris, M. Dimarogona, A. Karnaouri, E. Topakas, A. Karantonis, Direct electron  
21 transfer of lytic polysaccharide monoxygenases (LPMOs) and determination of their formal  
22 potentials by large amplitude Fourier transform alternating current cyclic voltammetry,  
23 *Bioelectrochemistry.* 124 (2018) 149–155. doi:10.1016/j.bioelechem.2018.07.009.

24

## 1 **Figure legends**

2 **Figure 1.** The activity of *TaAA9A* on phosphoric acid-swollen cellulose (PASC) in the  
3 presence of ascorbic acid (AscA) or spent sulfite liquor (SSL). High-performance anion  
4 exchange chromatography (HPAEC) traces show reaction products released from PASC (5 g/L)  
5 upon incubation with *TaAA9A* (1  $\mu$ M) in the presence of 1 mM AscA (orange lines) or 10 g/L  
6 SSL (blue lines). The black solid line represents PASC incubated with *TaAA9A* in the absence  
7 of reductant. Dashed lines represent PASC incubated in the presence of corresponding reductant  
8 and in the absence of LPMO. Reactions were carried out in 50 mM sodium acetate buffer pH  
9 5.0, at 50 °C, with orbital shaking at 750 rpm, for 24 h.

10 **Figure 2.** (A) Glucan to glucose conversion, (B) Glc4gemGlc concentration and (C) oxidation-  
11 reduction potential (ORP) during bioreactor enzymatic hydrolysis of sulfite-pretreated spruce at  
12 12% DM. Circle indicates 200  $\mu$ mol/Lh H<sub>2</sub>O<sub>2</sub> feed in aerobic conditions, triangle up indicates  
13 no H<sub>2</sub>O<sub>2</sub> feed in aerobic conditions, triangle down indicates 200  $\mu$ mol/Lh H<sub>2</sub>O<sub>2</sub> feed in  
14 anaerobic conditions and square indicates no H<sub>2</sub>O<sub>2</sub> feed in anaerobic conditions. H<sub>2</sub>O<sub>2</sub> feed was  
15 started at 16 h. Dashed lines indicate the 16 and 42 h time-points.

16 **Figure 3.** (A) Glucan to glucose conversion, (B) Glc4gemGlc concentration, (C) oxidation-  
17 reduction potential (ORP) and (D) amount of H<sub>2</sub>O<sub>2</sub> added during bioreactor enzymatic  
18 hydrolysis of sulfite-pretreated spruce at 12% DM with ORP-controlled H<sub>2</sub>O<sub>2</sub> feeding in  
19 anaerobic conditions. Circle indicates ORP set-point at -40 mV, triangle down indicates ORP  
20 set-point at -80 mV and triangle up indicates ORP set-point at -120 mV. The ORP control was  
21 started at 2 h.

22 **Figure 4.** (A) Glucan to glucose conversion, (B) Glc4gemGlc concentration, (C) oxidation-  
23 reduction potential (ORP) and (D) amount of H<sub>2</sub>O<sub>2</sub> added during bioreactor enzymatic  
24 hydrolysis of sulfite-pretreated spruce at 12% DM with ORP-controlled H<sub>2</sub>O<sub>2</sub> feeding in aerobic  
25 conditions. Circle indicates ORP control at 110 mV starting at 2 h, triangle down indicates ORP



1 control at 120 mV starting at 42 h and triangle up indicates ORP control ramp from 110 to 150  
2 mV. Dashed line indicates the 42 h time-point.

3 **Figure 5.** (A) Glucan to glucose conversion, (B) Glc4gemGlc concentration and (C) oxidation-  
4 reduction potential (ORP) during bioreactor enzymatic hydrolysis of sulfite-pretreated spruce at  
5 12% DM. Circle indicates a double dose of spent sulfite liquor (20 g/L SSL), triangle down  
6 indicates ORP controlled at 110 mV by SSL feeding and triangle up indicates a 2<sup>nd</sup> dose of  
7 Cellic CTec3 added at 42 h. All experiments were done in aerobic conditions with a 200  
8  $\mu\text{mol/Lh H}_2\text{O}_2$  feed starting at 16 h. Dashed lines indicate the 16 and 42 h time-points.  
9 Quantitative comparison of panels A and B allows an approximation of the fraction of oxidized  
10 products to be made; such a comparison shows that in the experiment with two dosages of  
11 Cellic CTec3, after 72 hours, there is approximately 1 oxidized dimer per 150 released glucose  
12 molecules.

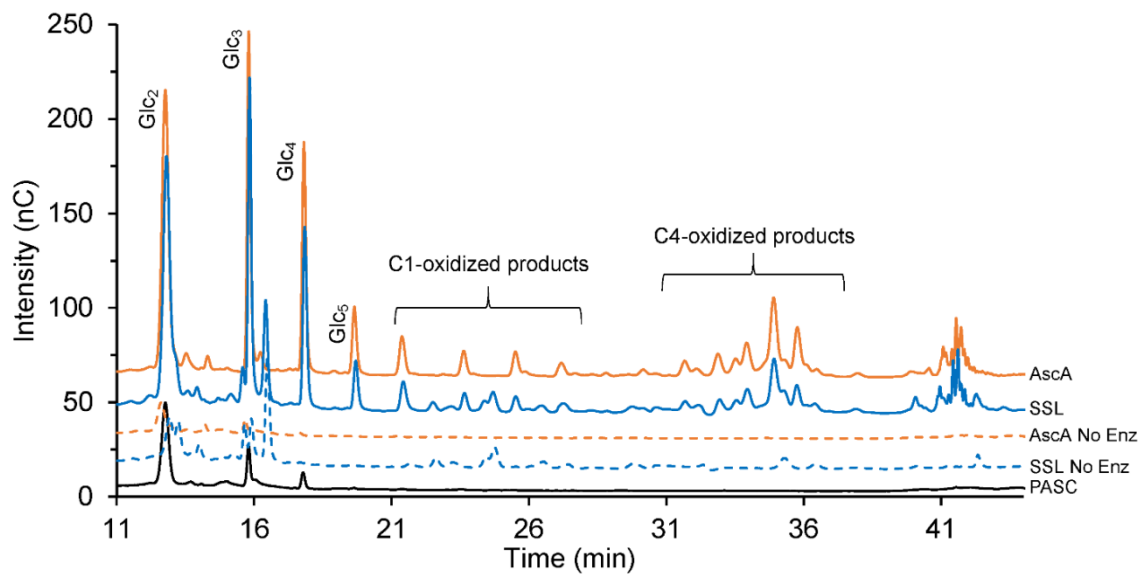
**Table 1.** Composition of the sulfite pretreated spruce solids and spent sulfite liquor (SSL). The percentages of sugars refer to anhydro sugars. The full composition of the SSL is proprietary information of Borregaard A/S.

|                          | <b>Pretreated spruce solids<br/>(% of DM<sup>†</sup>)</b> |           | <b>Dissolved sugars in SSL<br/>(g/L)</b> |
|--------------------------|---|-----------|--|
| Glucan                   | 87.4±0.6  | Glucose   | 6.02±0.05                                |
| Mannan                   | 5.2±0.2   | Mannose   | 20.66±0.61                               |
| Galactan                 | nd <sup>‡</sup>   | Galactose | 3.95±0.10                                |
| Xylan                    | 2.7±0.1   | Xylose    | 8.57±0.31                                |
| Arabinan                 | nd  | Arabinose | 1.44±0.05                                |
| Acid insoluble<br>lignin | 3.3±0.3   |           |  |

<sup>†</sup>dry-matter, <sup>‡</sup>not detected

1

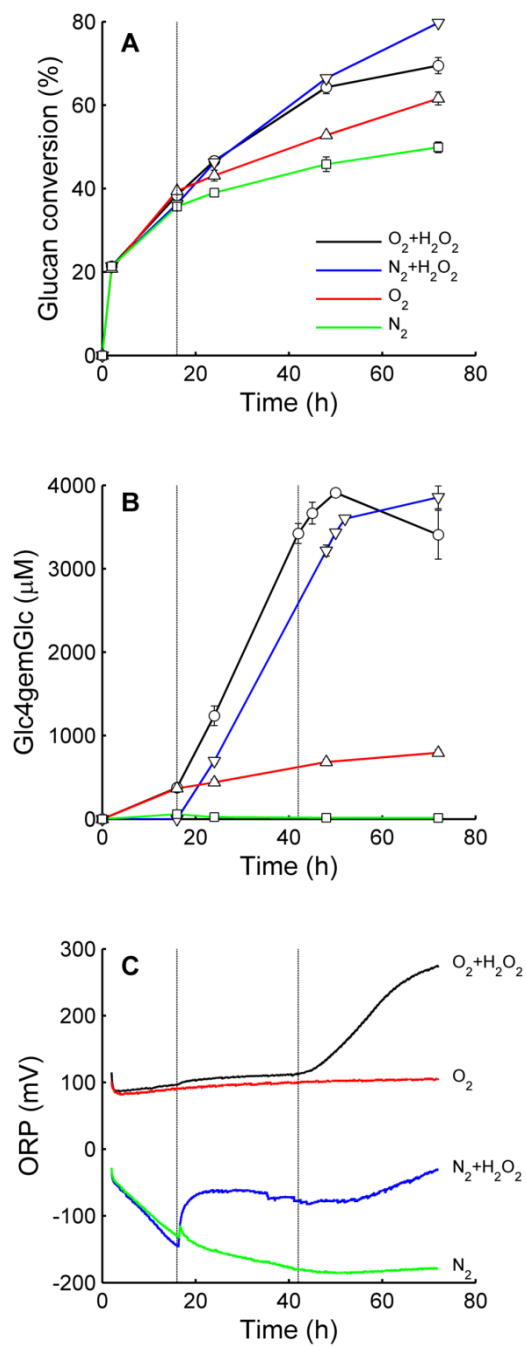
1 **Figure 1**



2

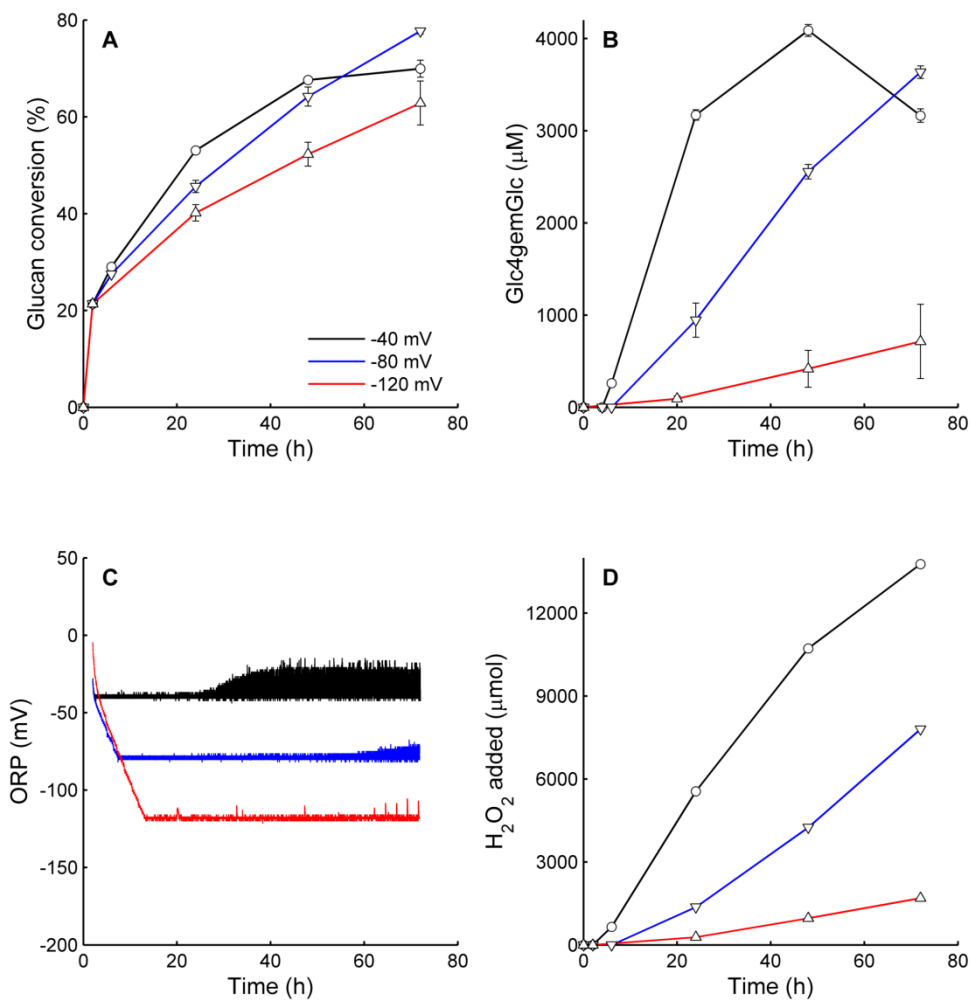
3

1 Figure 2



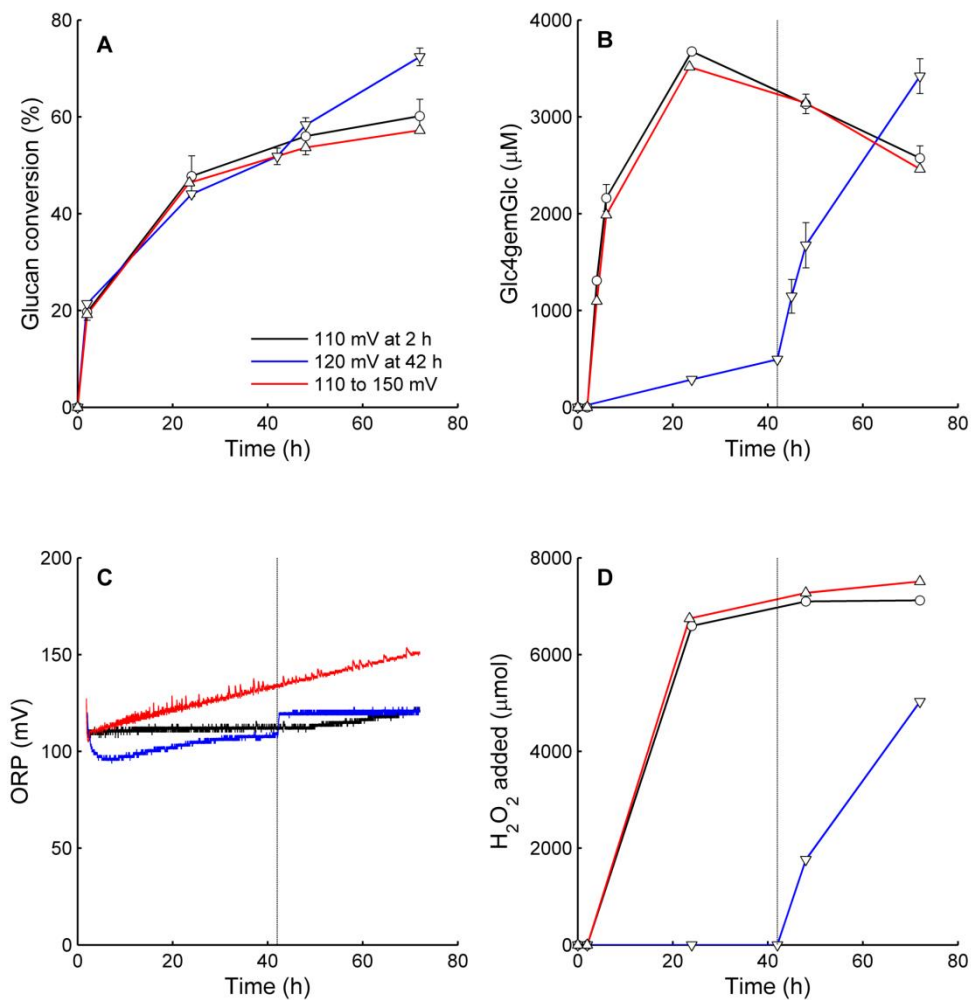
2

1 Figure 3



2  
3

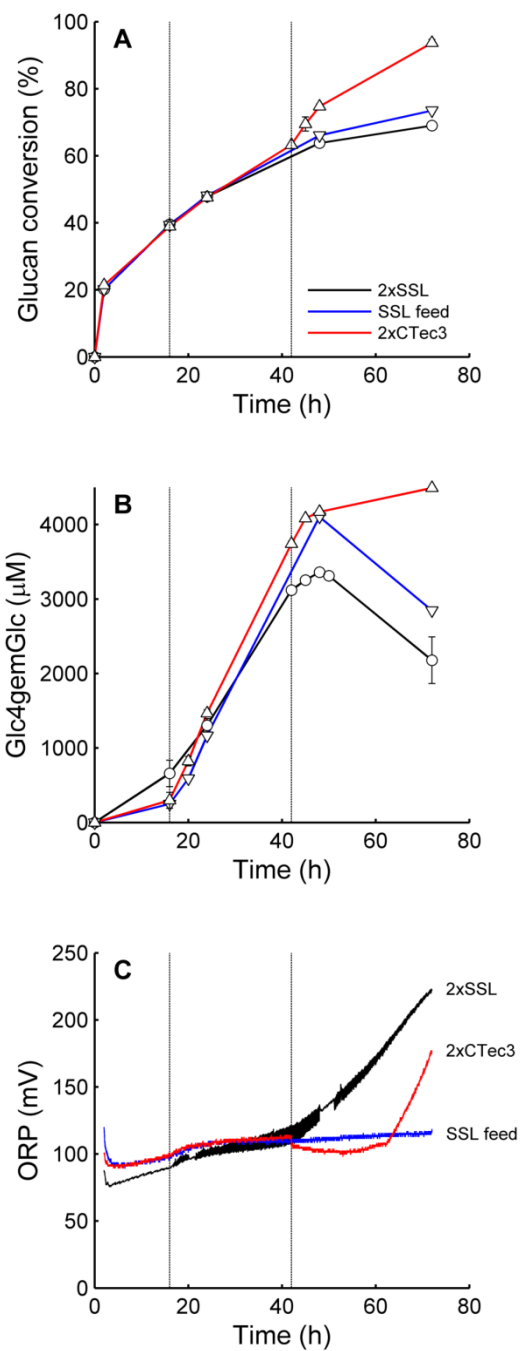
1 **Figure 4**



2

3

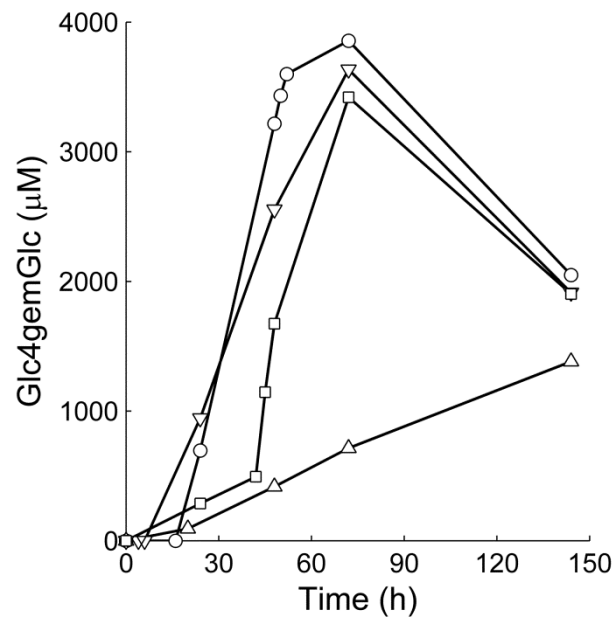
1 **Figure 5**



2

3

**Supplementary figure 1.** Glc4gemGlc concentration during bioreactor enzymatic hydrolysis of sulfite-pretreated spruce at 12% DM. Circle represents 200  $\mu\text{mol/Lh}$   $\text{H}_2\text{O}_2$  feed in anaerobic conditions. Triangle down represents ORP-controlled  $\text{H}_2\text{O}_2$  feeding in anaerobic conditions with ORP set at -80 mV. Triangle up represents ORP-controlled  $\text{H}_2\text{O}_2$  feeding in anaerobic conditions with ORP set at -120 mV. Square represents ORP-controlled  $\text{H}_2\text{O}_2$  feeding in aerobic conditions with ORP set at 120 mV starting at 42 h.





**Supplementary figure 2.** Oxidation-reduction potential (ORP) during control experiments with sulfite pretreated spruce (1% DM), 10 g/L spent sulfite liquor (SSL) and no added enzyme. Black line indicates 200  $\mu\text{mol/Lh}$   $\text{H}_2\text{O}_2$  feed in aerobic conditions and blue line indicates 200  $\mu\text{mol/Lh}$   $\text{H}_2\text{O}_2$  feed in anaerobic conditions. Dashed line indicates the start of  $\text{H}_2\text{O}_2$  feed at 16 h.

